Dynamical symmetries and beyond: Lessons and advances

Cite as: AIP Conference Proceedings **2150**, 020013 (2019); https://doi.org/10.1063/1.5124585
Published Online: 03 September 2019

A. Leviatan

Dynamical Symmetries and Beyond: Lessons and Advances

A. Leviatan

Racah Institute of Physics, The Hebrew University, Jerusalem 91904, Israel

Corresponding author: ami@phys.huji.ac.il
URL: http://www.phys.huji.ac.il/~ami/

Abstract. A central theme in Iachello's quest for understanding simple ordered patterns in complex quantum systems, is the concept of dynamical symmetry. Relying on his seminal contributions, we present further generalization of this notion to that of partial dynamical symmetry (PDS), for which solvability and good quantum numbers are maintained by only a subset of states. Hamiltonians with a single PDS and multiple PDSs are constructed explicitly and their relevance to nuclear structure is discussed.

INTRODUCTION

The concept of dynamical symmetry (DS) is now widely recognized to play a pivotal role in our understanding of dynamical systems. In particular, it had a major impact on developments in nuclear [1, 2], molecular [3] and hadronic physics [4], pioneered by F. Iachello and his colleagues. Its basic paradigm is to write the Hamiltonian of the system,

$$\hat{H}_{\rm DS} = \sum_G a_G\, \hat{C}[G] \qquad\qquad E_{\rm DS}(\lambda_{\rm dyn},\, \lambda_1,\, \lambda_2,\, \ldots,\, \lambda_{\rm sym})\,, \tag{1}$$

in terms of the Casimir operators, $\hat{C}[G]$, of a chain of nested algebras [5],

$$G_{\rm dyn} \supset G_1 \supset G_2 \supset \ldots \supset G_{\rm sym} \qquad\qquad |\lambda_{\rm dyn},\, \lambda_1,\, \lambda_2,\, \ldots,\, \lambda_{\rm sym}\rangle\,. \tag{2}$$

In such a case, the spectrum is completely solvable, the eigenstates and energies, $E_{\rm DS}$, are labeled by quantum numbers $(\lambda_{\rm dyn},\, \lambda_1,\, \lambda_2,\, \ldots,\, \lambda_{\rm sym})$, which are the labels of irreducible representations (irreps) of the algebras in the chain. In Eq. (2), $G_{\rm dyn}$ is the dynamical (spectrum generating) algebra of the system such that operators of all physical observables can be written in terms of its generators and $G_{\rm sym}$ is the symmetry algebra. A given $G_{\rm dyn}$ can encompass several DS chains, each providing characteristic analytic expressions for observables and definite selection rules.

A notable example of such algebraic construction is the interacting boson model (IBM) [6, 7, 8, 9], describing low-lying quadrupole collective states in nuclei in terms of N monopole (s) and quadrupole (d) bosons, representing valence nucleon pairs. The model is based on a unitary spectrum generating algebra $G_{\rm dyn} = {\rm U}(6)$ and an orthogonal (angular-momentum) symmetry algebra $G_{\rm sym} = {\rm SO}(3)$. The Hamiltonian is expanded in the elements of U(6), and consists of Hermitian, rotational-scalar interactions which conserve the total number of s- and d- bosons, $\hat{N} = \hat{n}_s + \hat{n}_d = s^\dagger s + \sum_m d^\dagger_m d_m$. The solvable limits of the IBM correspond to the following DS chains,

$$\begin{aligned}
&{\rm U}(6) \supset {\rm U}(5) \supset {\rm SO}(5) \supset {\rm SO}(3) && |N,\, n_d,\, \tau,\, n_\Delta,\, L\rangle && E_{\rm DS} = \epsilon_d\, n_d + A\, n_d(n_d+4) + B\,\tau(\tau+3) + C\,L(L+1)\,, && (3)\\
&{\rm U}(6) \supset {\rm SU}(3) \supset {\rm SO}(3) && |N,\, (\lambda,\mu),\, K,\, L\rangle && E_{\rm DS} = A(\lambda^2+\mu^2+\lambda\mu+3\lambda+3\mu) + C\,L(L+1)\,, && (4)\\
&{\rm U}(6) \supset \overline{{\rm SU}(3)} \supset {\rm SO}(3) && |N,\, (\bar\lambda,\bar\mu),\, \bar K,\, L\rangle && E_{\rm DS} = A(\bar\lambda^2+\bar\mu^2+\bar\lambda\bar\mu+3\bar\lambda+3\bar\mu) + C\,L(L+1)\,, && (5)\\
&{\rm U}(6) \supset {\rm SO}(6) \supset {\rm SO}(5) \supset {\rm SO}(3) && |N,\, \sigma,\, \tau,\, n_\Delta,\, L\rangle && E_{\rm DS} = A\,\sigma(\sigma+4) + B\,\tau(\tau+3) + C\,L(L+1)\,. && (6)
\end{aligned}$$

Here $N, n_d, (\lambda,\mu), (\bar\lambda,\bar\mu), \sigma, \tau, L$, label the relevant irreps of U(6), U(5), SU(3), $\overline{\rm SU(3)}$, SO(6), SO(5), SO(3), respectively, and $n_\Delta, K, \bar K$ are multiplicity labels. Each chain provides a complete basis whose members are eigenstates of the Casimir operators in the chain with eigenvalues listed above. The resulting spectra of these DS chains with

Symmetries and Order: Algebraic Methods in Many Body Systems
AIP Conf. Proc. 2150, 020013-1–020013-10; https://doi.org/10.1063/1.5124585
Published by AIP Publishing. 978-0-7354-1895-0/$30.00

leading sub-algebras G_1: U(5), SU(3), $\overline{\text{SU(3)}}$ and SO(6), resemble known paradigms of nuclear collective structure: spherical vibrator, prolate-, oblate- and γ-soft deformed rotors, respectively. Electromagnetic moments and rates can be calculated with transition operators of appropriate rank. For example, the one-body $E2$ operator reads $\hat{T}(E2) = e_B[d^\dagger s + s^\dagger \tilde{d} + \chi\,(d^\dagger \tilde{d})^{(2)}]$, where $\tilde{d}_m = (-1)^m d_{-m}$, and standard notation of angular momentum coupling is used.

A geometric visualization of the IBM is obtained by an energy surface,

$$E_N(\beta,\gamma) \quad = \quad \langle \beta,\gamma; N|\hat{H}|\beta,\gamma; N\rangle \ , \tag{7}$$

defined by the expectation value of the Hamiltonian in a coherent (intrinsic) state [10, 11]. Here (β,γ) are quadrupole shape parameters whose values, $(\beta_{\rm eq},\gamma_{\rm eq})$, at the global minimum of $E_N(\beta,\gamma)$ define the equilibrium shape for a given Hamiltonian. The shape can be spherical ($\beta=0$) or deformed ($\beta>0$) with $\gamma=0$ (prolate), $\gamma=\pi/3$ (oblate), $0<\gamma<\pi/3$ (triaxial) or γ-independent. The equilibrium deformations associated with the DS limits of Eqs. (3)-(6), conform with their geometric interpretation, and are given by $\beta_{\rm eq}=0$ for U(5), ($\beta_{\rm eq}=\sqrt{2}, \gamma_{\rm eq}=0$) for SU(3), ($\beta_{\rm eq}=\sqrt{2}, \gamma_{\rm eq}=\pi/3$) for $\overline{\text{SU(3)}}$, and ($\beta_{\rm eq}=1$, $\gamma_{\rm eq}$ arbitrary) for SO(6). The DS Hamiltonians support a single minimum in their energy surface, hence serve as benchmarks for the dynamics of a single quadrupole shape.

Since its introduction, the IBM has been the subject of many investigations, becoming a standard model for the description of atomic nuclei. An important lesson from these extensive studies is the observation that, although a dynamical symmetry provides considerable insights, in most applications to realistic systems, the predictions of an exact DS are rarely fulfilled and one is compelled to break it. More often one finds that the assumed symmetry is not obeyed uniformly, *i.e.*, is fulfilled by some of the states but not by others. The need to address such situations, but still preserve important symmetry remnants, has motivated the introduction of partial dynamical symmetry (PDS) [12]. The essential idea is to relax the stringent conditions of *complete* solvability so that only part of the eigenspectrum retains analyticity and/or good quantum numbers. The novel notion of PDS and its implications to nuclear structure are the subject matter of the present contribution.

PARTIAL DYNAMICAL SYMMETRY AND NUCLEAR SPECTROSCOPY

A partial dynamical symmetry (PDS) corresponds to a particular symmetry-breaking for which the virtues of a dynamical symmetry (DS), namely, solvability and good quantum numbers, are fulfilled by only a subset of states. The IBM, with its rich algebraic structure, provides a convenient framework for realizing the PDS notion and testing its predictions. Consider one of the DS chains of the IBM, Eqs. (3)-(6),

$$\text{U(6)} \supset \text{G}_1 \supset \text{G}_2 \supset \ldots \supset \text{SO(3)} \qquad\qquad |N,\ \lambda_1,\ \lambda_2,\ \ldots,\ L\rangle \ , \tag{8}$$

with leading sub-algebra G_1 and basis $|N,\lambda_1,\lambda_2,\ldots,L\rangle$. The algorithm for constructing Hamiltonians with PDS, associated with the reduction (8), is based on identifying n-particle annihilation operators $\hat{T}_\alpha$ which satisfy [13, 14],

$$\hat{T}_\alpha|N,\lambda_1=\Lambda_0,\lambda_2,\ldots,L\rangle = 0 \ . \tag{9}$$

The set of states in Eq. (9) are basis states of a particular G_1-irrep, $\lambda_1=\Lambda_0$, with good G_1 symmetry, and are specified by the quantum numbers of the algebras in the chain (8). These states may span the entire or part of the indicated irrep. Condition (9) ensures that they are zero-energy eigenstates of the following normal-ordered Hamiltonian,

$$\hat{H} \quad = \quad \sum_{\alpha,\beta} u_{\alpha\beta}\hat{T}^\dagger_\alpha \hat{T}_\beta \ . \tag{10}$$

$\hat{H}$ itself, however, need not be invariant under G_1 and, therefore, has partial-G_1 symmetry. The degeneracy of the above set of states is lifted, without affecting their wave functions, by adding to $\hat{H}$ the following Hamiltonian

$$\hat{H}_c \quad = \quad \sum_{G_i\subset G_1} a_{G_i}\hat{C}[G_i] \ , \tag{11}$$

composed of the Casimir operators of the sub-algebras of G_1 in the chain (8). The states $|N,\lambda_1=\Lambda_0,\lambda_2,\ldots,L\rangle$ remain solvable eigenstates of the complete Hamiltonian

$$\hat{H}_{\rm PDS} \quad = \quad \hat{H} + \hat{H}_c \ , \tag{12}$$

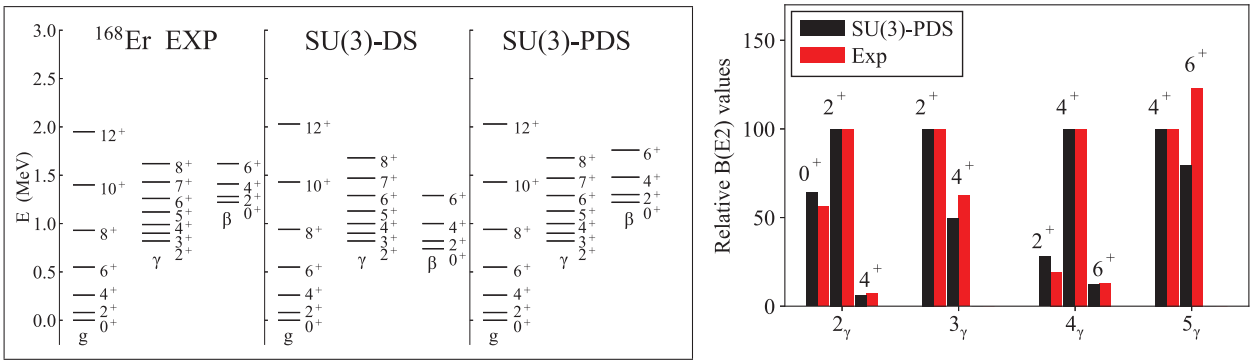

FIGURE 1. Left panels: observed spectrum of ^{168}Er compared with SU(3)-DS and SU(3)-PDS calculations. The latter employs $\hat{H}_{\rm PDS}$ of Eq. (18) with $h_0 = 8$, $h_2 = 4$, $C = 13$ keV and $N = 16$. Right panel: comparison of the PDS parameter-free predictions with the data on the relative $B(E2; L_\gamma \to L)$ values for $\gamma \to g$ $E2$ transitions in ^{168}Er. Adapted from [17, 19].

which, by definition, has G_1-PDS. In the nuclear physics terminology, the decomposition of Eq. (12) is referred to as a resolution of the Hamiltonian into intrinsic ($\hat{H}$) and collective ($\hat{H}_c$) parts [15, 16]. The former determines the energy surface (7) and band-structure, while the latter determines the in-band rotational splitting. Since $\hat{H}$ is related to the Casimir operator of G_1 for a specific choice of parameters, the PDS-Hamiltonian of Eq. (12) can be also transcribed in the form

$$\hat{H}_{\rm PDS} \quad = \quad \hat{H}_{\rm DS} + \hat{V}_0 \,, \tag{13}$$

where $\hat{H}_{\rm DS}$ is the DS Hamiltonian, Eq. (1), for the chain (8) and $\hat{V}_0$ satisfies $\hat{V}_0|N, \lambda_1 = \Lambda_0, \lambda_2, \ldots, L\rangle = 0$. In what follows, we present explicit PDS Hamiltonians associated with the DS chains of the IBM, and show their relevance to nuclear spectroscopy.

The spectrum corresponding to the SU(3)-DS chain of Eq. (4), resembles that of a prolate-deformed roto-vibrator. The eigenstates are arranged in SU(3) (λ, μ)-multiplets, forming rotational K-bands with characteristic $L(L+1)$ splitting. The label K corresponds geometrically to the projection of the angular momentum on the symmetry axis. The lowest SU(3) irrep $(2N, 0)$ contains the ground band g($K = 0$), and the irrep $(2N-4, 2)$ contains both the $\beta(K = 0)$ and $\gamma(K = 2)$ bands.

The construction of Hamiltonians with SU(3)-PDS follows the general algorithm. The two-boson pair operators

$$P^\dagger_0 \quad = \quad d^\dagger \cdot d^\dagger - 2(s^\dagger)^2 \,, \tag{14}$$

$$P^\dagger_{2m} \quad = \quad 2d^\dagger_m s^\dagger + \sqrt{7}\,(d^\dagger\, d^\dagger)^{(2)}_m \,, \tag{15}$$

are $(\lambda, \mu) = (0, 2)$ tensors of SU(3), and annihilate all L-states of the SU(3) ground band irrep $(\lambda, \mu) = (2N, 0)$,

$$\begin{aligned} P_0\,|N,\,(\lambda,\mu)=(2N,0),\,K=0,\,L\rangle \quad &= \quad 0\,, \qquad\qquad L = 0, 2, 4 \ldots, 2N \\ P_{2m}\,|N,\,(\lambda,\mu)=(2N,0),\,K=0,\,L\rangle \quad &= \quad 0\,. \end{aligned} \tag{16}$$

In addition, P_0 satisfies

$$P_0\,|N,\,(\lambda,\mu)=(2N-4k,2k),\,K=2k,\,L\rangle = 0\,, \quad L = K, K+1, \ldots, (2N-2k)\,. \tag{17}$$

For $k > 0$, the L-states of Eq. (17) span only part of the SU(3) irreps $(\lambda, \mu) = (2N-4k, 2k)$ and form the rotational members of excited $\gamma^k(K = 2k)$ bands. P_0 and P_{2m} correspond to the operators $\hat{T}_\alpha$ of Eq. (9). The intrinsic Hamiltonian reads $\hat{H} = h_0\, P^\dagger_0 P_0 + h_2\, P^\dagger_2 \cdot \tilde{P}_2$, where $\tilde{P}_{2m} = (-)^m P_{2,-m}$ and the centered dot denotes a scalar product. The collective Hamiltonian, $\hat{H}_c = C\,\hat{C}_2[{\rm SO}(3)]$, is composed of the quadratic Casimir operator of SO(3), with eigenvalues $L(L+1)$. The complete Hamiltonian with SU(3)-PDS has the form as in Eqs. (12) and (13), and is given by [17],

$$\hat{H}_{\rm PDS} = h_0 P^\dagger_0 P_0 + h_2 P^\dagger_2 \cdot \tilde{P}_2 + C\,\hat{C}_2[{\rm SO}(3)] = \hat{\rm H}_{\rm SU(3)-DS} + \eta_0\,{\rm P}^\dagger_0 {\rm P}_0\,. \tag{18}$$

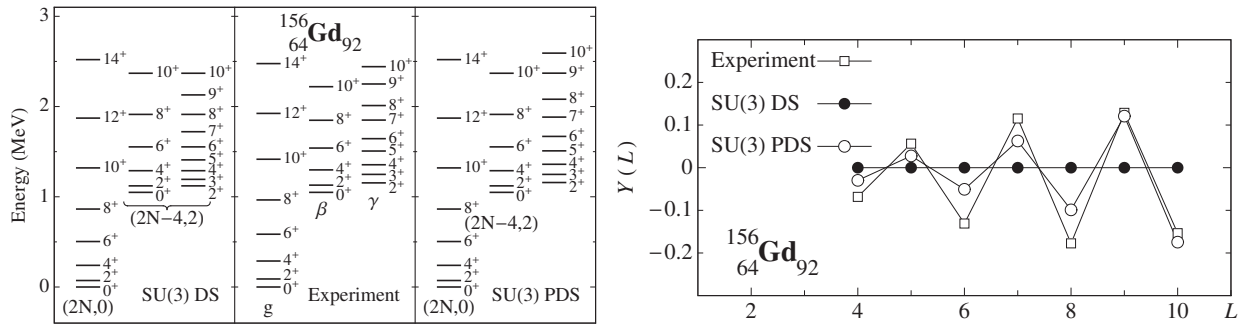

FIGURE 2. Observed spectrum of ^{156}Gd (left panels) and odd-even staggering of the γ band (right panel), compared with SU(3)-DS and SU(3)-PDS calculations. The latter employs $\hat{H}_{\rm PDS}$ of Eq. (22) with $A=-7.6$, $C=12$, $\eta_2=-18.1$, $\eta_3=46.2$ keV and $N=12$. Here $Y(L)=\frac{2L-1}{L}\times\frac{E(L)-E(L-1)}{E(L)-E(L-2)}-1$, where $E(L)$ is the energy of a γ-band level with angular momentum L. Adapted from [21].

The second equality in Eq. (18) follows from the fact that for $h_2=h_0$, the combination $P_0^\dagger P_0+P_2^\dagger\cdot\tilde{P}_2=-\hat{C}_2[{\rm SU(3)}]+2\hat{N}(2\hat{N}+3)$ is related to the quadratic Casimir operator of SU(3), hence can be assigned to the DS-Hamiltonian, $\hat{H}_{\rm SU(3)-DS}$, of Eq. (4). In general, $\hat{H}_{\rm PDS}$ of Eq. (18) has SU(3)-PDS with solvable ground $g(K=0)$ and $\gamma^k(K=2k)$ bands of good SU(3) symmetry, while other bands, in particular the $\beta(K=0)$ band, are mixed.

The experimental spectra of the ground $g(K=0)$, $\gamma(K=2)$ and $\beta(K=0)$ bands in ^{168}Er is shown in Fig. 1, and compared with an exact DS ($\eta_0=0$) and PDS ($\eta_0\neq 0$) calculations [17]. The SU(3) PDS spectrum is clearly seen to be an improvement over the exact SU(3) DS description, since the β-γ degeneracy is lifted. The ground and gamma are still pure SU(3) bands, but the beta band is found to contain 13% admixtures into the dominant $(2N-4,2)$ irrep [18]. Since the wave functions of the solvable states are known, it is possible to obtain *analytic* expressions for matrix elements of observables between them. The $E2$ operator can be transcribed as $\hat{T}(E2)=\alpha\,Q^{(2)}+\theta\,(d^\dagger s+s^\dagger\tilde{d})$, with $Q^{(2)}$ an SU(3) generator. Since the solvable ground and gamma bands reside in different SU(3) irreps, $Q^{(2)}$ cannot connect them and, consequently, $B(E2)$ ratios for $\gamma\rightarrow g$ transitions do no depend on the $E2$ parameters (α,θ) nor on parameters of the PDS Hamiltonian (18). Overall, as shown in the right panel of Fig. 1, these parameter-free predictions of SU(3)-PDS account well for the data in ^{168}Er. Similar evidence for SU(3)-PDS has been presented by Casten *et. al.* for other rare-earth and actinide nuclei [19, 20], suggesting a wider applicability of this concept.

Another class of Hamiltonians with SU(3) PDS exists, constructed of the following three-boson operators,

$$W^\dagger_{3m} = (P^\dagger_2\,d^\dagger)^{(3)}_m=\sqrt{7}\,[(d^\dagger d^\dagger)^{(2)}d^\dagger]^{(3)}_m\,, \tag{19}$$

$$W^\dagger_{4m} = (P^\dagger_2\,d^\dagger)^{(4)}_m\,, \tag{20}$$

where $P^\dagger_{2m}$ is given in Eq. (15). The $W^\dagger_{\ell m}$ operators are $(2,2)$ tensors under SU(3) and satisfy,

$$\begin{aligned} W_{\ell m}\,|N,\,(\lambda,\mu)=(2N,0),\,K=0,\,L\rangle &= 0\,, \qquad \ell=2,3\\ W_{\ell m}\,|N,\,(\lambda,\mu)=(2N-4,2),\,K=0,\,L\rangle &= 0\,. \end{aligned} \tag{21}$$

The above indicated states span the irrep $(2N,0)$ and part of the irrep $(2N-4,2)$ of SU(3). The resulting SU(3)-PDS Hamiltonian has the form [21],

$$\hat{H}_{\rm PDS}=\hat{H}_{\rm SU(3)-DS}+\eta_2\,W^\dagger_2\cdot\tilde{W}_2+\eta_3\,W^\dagger_3\cdot\tilde{W}_3\,, \tag{22}$$

where $\hat{H}_{\rm SU(3)-DS}$ is the SU(3)-DS Hamiltonian of Eq. (4). Relations (21) ensure that $\hat{H}_{\rm PDS}$ has solvable ground and β bands with good SU(3) symmetry, while other bands, in particular the γ band, are mixed.

A comparison of the experimental spectrum of ^{156}Gd with the SU(3)-DS calculation in Fig. 2, shows a good description for properties of states in the ground and β bands, however, the resulting fit to energies of the γ-band is quite poor. The latter are not degenerate with the β band and, moreover, display an odd-even staggering with pronounced deviations from a rigid-rotor $L(L+1)$ pattern. This effect can be visualized by plotting the quantity $Y(L)$, defined in the caption of Fig. 2. For a rotor this quantity is flat, $Y(L)=0$, as illustrated in the right panel of Fig. 2 with the SU(3) DS calculation, which is in marked disagreement with the empirical data. In the PDS calculation, the gamma

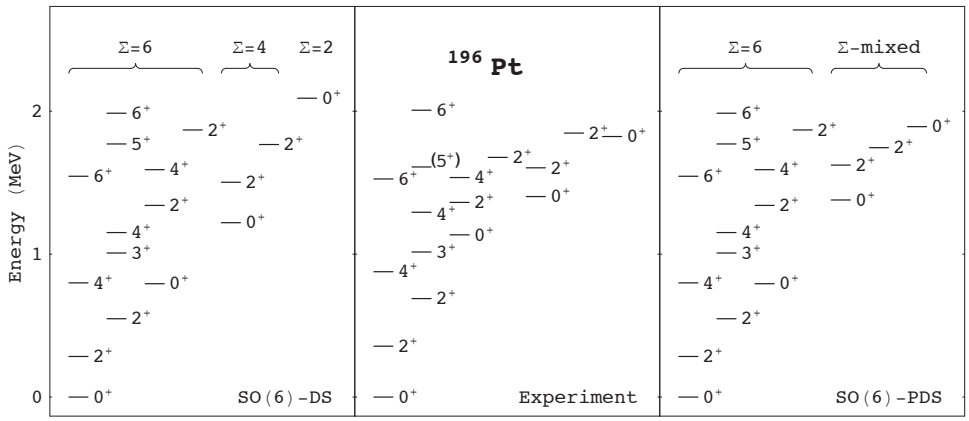

FIGURE 3. Observed spectrum of ^{196}Pt compared with SO(6)-DS and SO(6)-PDS calculations. The latter employs $\hat{H}_{\rm PDS}$ of Eq. (24) with $r_0 = 16.41$, $r_2 = 7.68$, $B = 44.0$, $C = 17.9$ keV and $N = 6$. Σ is an SO(6) label. Adapted from [14].

band contains 15% SU(3) admixtures into the dominant $(2N-4, 2)$ irrep and the empirical odd-even staggering is well reproduced. The PDS results for the γ band are obtained without affecting the solvability and SU(3) purity of states in the ground and beta bands. Since for the latter states the wave functions are known, one has at hand closed expressions for $E2$ transitions between them that can be used as tests for SU(3)-PDS. Recent measurements by Aprahamian *et. al.* of lifetimes for $E2$ decays from states of the β-band in ^{156}Gd [22], confirm the PDS predictions.

The spectrum corresponding to the SO(6)-DS chain of Eq. (6), resembles that of a γ-unstable deformed roto-vibrator, where states are arranged in SO(6) multiplets with $\sigma = N - 2v$ ($v = 0, 1, 2, \ldots$), and exhibit $\tau(\tau+3)$ and $L(L+1)$ rotational splitting. To construct Hamiltonians with SO(6)-PDS, we consider the three-boson operators $s^\dagger R_0^\dagger$ and $d_m^\dagger R_0^\dagger$, where $R_0^\dagger = d^\dagger \cdot d^\dagger - (s^\dagger)^2$. These $\sigma = 1$ tensors of SO(6) annihilate all (τ, n_Δ, L) states in the irrep $\sigma = N$,

$$\begin{aligned} sR_0\,|N, \sigma = N, \tau, n_\Delta, L\rangle &= 0\,, \qquad \tau = 0, 1, 2, \ldots, N \\ d_m R_0\,|N, \sigma = N, \tau, n_\Delta, L\rangle &= 0\,. \end{aligned} \tag{23}$$

The intrinsic Hamiltonian reads $\hat{H} = r_0\, R_0^\dagger \hat{n}_s R_0 + r_2\, R_0^\dagger \hat{n}_d R_0$ and the collective Hamiltonian is composed of the quadratic Casimir operators of SO(5) and SO(3). The complete Hamiltonian with SO(6)-PDS has the form [14],

$$\hat{H}_{\rm PDS} = r_0\, R_0^\dagger \hat{n}_s R_0 + r_2\, R_0^\dagger \hat{n}_d R_0 + B\,\hat{C}_2[{\rm SO(5)}] + {\rm C}\,\hat{\rm C}_2[{\rm SO(3)}] = \hat{\rm H}_{\rm SO(6)-DS} + \eta\, {\rm R}_0^\dagger \hat{\rm n}_{\rm s} {\rm R}_0\,, \tag{24}$$

where the last equality follows from the fact that for $r_2 = r_0$, the intrinsic Hamiltonian is related to the Casimir operator of SO(6), $R_0^\dagger R_0 = -\hat{C}_2[{\rm SO(6)}] + \hat{N}(\hat{N}+4)$, hence can be assigned to the DS-Hamiltonian, $\hat{H}_{\rm SO(6)-DS}$, of Eq. (6).

A comparison with the experimental spectrum of ^{196}Pt in Fig. 3 and available $E2$ rates, reveals that the SO(6)-DS limit provides a good description for properties of states in the ground band. However, the resulting fit to energies of excited bands is quite poor. The 0_1^+, 0_3^+, and 0_4^+ levels of ^{196}Pt at excitation energies 0, 1403, 1823 keV, respectively, are identified as the bandhead states of the ground ($v = 0$), first- ($v = 1$) and second- ($v = 2$) excited β-vibrational bands. Their empirical anharmonicity, defined by the ratio $R = E(v=2)/E(v=1) - 2$, is found to be $R = -0.70$. The SO(6)-DS value is $R = -0.29$, in marked disagreement with the empirical value. For the SO(6)-PDS Hamiltonian (24), the ground band remains solvable with good SO(6) symmetry ($\sigma = N$), while the excited bands exhibit strong SO(6) breaking. The calculated PDS anharmonicity is $R = -0.63$, much closer to the empirical value [14].

The spectrum corresponding to the U(5)-DS chain of Eq. (3), resembles that of a spherical vibrator, where states are arranged in U(5) multiplets: $(n_d = L = 0)$, $(n_d = 1, L = 2)$, $(n_d = 2, L = 4, 2, 0)$ and $(n_d = 3, L = 6, 4, 3, 0, 2)$, with strong connecting $n_d + 1 \to n_d$ $E2$ transitions. The U(5) basis states $|N,\, n_d,\, \tau,\, n_\Delta,\, L\rangle$ have definite d-boson number n_d and seniority τ, and n_Δ counts the maximum number of d-boson triplets coupled to $L = 0$. The construction of Hamiltonians with U(5)-PDS follows the general algorithm. The three-boson operators, $G_0^\dagger = [(d^\dagger d^\dagger)^{(2)} d^\dagger]^{(0)}$ and $K_0^\dagger = s^\dagger (d^\dagger d^\dagger)^{(0)}$ are, respectively, $n_d = 3$ and $n_d = 2$ tensors with respect to U(5), and satisfy

$$\begin{aligned} G_0|N, n_d = \tau, \tau, n_\Delta = 0, L\rangle &= 0\,, \qquad L = \tau, \tau+1, \ldots, 2\tau-2, 2\tau \\ K_0|N, n_d = \tau, \tau, n_\Delta = 0, L\rangle &= 0\,. \end{aligned} \tag{25}$$

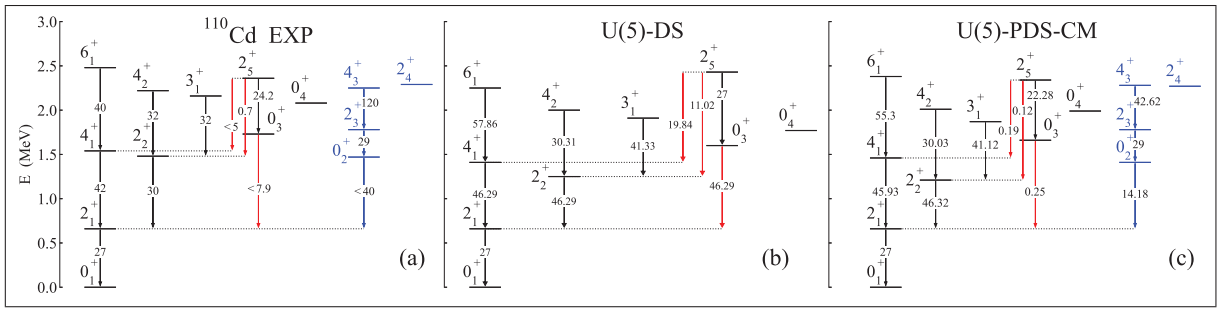

FIGURE 4. Experimental spectrum and representative $E2$ rates (in W.u.) of normal and intruder levels (0^+_2, 2^+_3, 4^+_3, 2^+_4) in ^{110}Cd, compared with U(5)-DS and U(5)-PDS calculations. The latter employs $\hat{H}_{\rm PDS}$ of Eq. (26) with parameters $\epsilon_d = 473.35$, $A = -B = 73.62$, $C = 18.47$, $r_0 = 2.15$, $e_0 = -6.92$ keV and $N = 7$ in the normal sector. The complete Hamiltonian contains additional interactions acting in the intruder sector and a small configuration-mixing (CM) term, see Ref. [23] for more details.

The resulting U(5)-PDS Hamiltonian contains the U(5)-DS Hamiltonian (3) and terms constructed of G_0 and K_0 [23],

$$\hat{H}_{\rm PDS} = \hat{H}_{\rm U(5)-DS} + r_0\, G^\dagger_0 G_0 + e_0 \left(G^\dagger_0 K_0 + K^\dagger_0 G_0\right) . \tag{26}$$

$\hat{H}_{\rm PDS}$ has the U(5) basis states of Eq. (25) as eigenstates, with energies as in Eq. (3), while other states are mixed.

The empirical spectrum of ^{110}Cd, shown in Fig. 4(a), consists of both normal and intruder levels, the latter based on 2p-4h proton excitations across the $Z = 50$ closed shell. A comparison of the calculated spectrum [Fig. 4((b)] and $B(E2)$ values obtained from the DS limit (3), demonstrates that most normal states have good spherical-vibrator properties and conform well with the properties of U(5)-DS. However, the measured rates for $E2$ decays from the non-yrast states, 0^+_3 ($n_d = 2$) and [0^+_4, 2^+_5 ($n_d = 3$)], reveal marked deviations from this behavior. In particular, $B(E2;\, 0^+_3 \to 2^+_1) < 7.9$, $B(E2;\, 2^+_5 \to 4^+_1) < 5$, $B(E2;\, 2^+_5 \to 2^+_2) = 0.7^{+0.5}_{-0.6}$ Weisskopf units (W.u.), are extremely small compared to the U(5)-DS values: 46.29, 19.84, 11.02 W.u., respectively. In a recent work [23], $\hat{H}_{\rm PDS}$ of Eq. (26) was taken to be the Hamiltonian in the normal sector with a small mixing to the intruder sector, in the framework of the interacting boson model with configuration mixing (IBM-CM). The resulting spectra, shown in Fig. 4(c), provides a good description of the empirical data in ^{110}Cd. The majority of normal yrast states in the spectrum, correspond to the states of Eq. (25), and maintain the good U(5) symmetry, to a good approximation. In contrast, the U(5) structure of the non-yrast states changes dramatically. The resulting calculated values: $B(E2;\, 0^+_3 \to 2^+_1) = 0.25$, $B(E2;\, 2^+_5 \to 4^+_1) = 0.19$ and $B(E2;\, 2^+_5 \to 2^+_2) = 0.12$ W.u., are consistent with the measured values [23].

MULTIPLE PARTIAL DYNAMICAL SYMMETRIES AND SHAPE COEXISTENCE

Symmetry plays a profound role in quantum phase transitions (QPTs), which are qualitative changes in the structure of a physical system, induced by a variation of a coupling constant in the quantum Hamiltonian. Such ground state phase transitions [24], are a pervasive phenomenon observed in many branches of physics [25], and are realized empirically in nuclei as transitions between different shapes [26, 27, 28, 29]. QPTs occur as a result of competing terms in the Hamiltonian with incompatible (non-commuting) symmetries. An interesting question to address is whether there are any symmetries (or traces of) still present in such circumstances, especially at the critical point where the structure changes most rapidly and mixing effects are enhanced. The feasibility of such persisting symmetries gained support from the works by Iachello on "critical-point symmetries" [30, 31], which demonstrated that the dynamics in such environment is amenable to *analytic* descriptions. A convenient framework to study symmetry-aspects of QPT in nuclei is the IBM [1], whose dynamical symmetries, Eqs. (3)-(6), correspond to possible phases of the system. The relevant Hamiltonians mix terms from different DS chains, $\hat{H}(\xi) \propto (1-\xi)\hat{H}_1 + \xi\,\hat{H}_2$. The nature of the phase transition is governed by the topology of the corresponding surface (7), which serves as a Landau's potential, with the equilibrium deformations as order parameters, and the coupling constant ξ as a control parameter. In the present contribution, we focus on remaining symmetries at the critical points of first-order QPTs, where the underlying surface exhibits multiple degenerate minima, with different types of dynamics (and symmetry) associated with each minimum. In such circumstances, exact DSs are broken and surviving symmetries, if any, are at most partial.

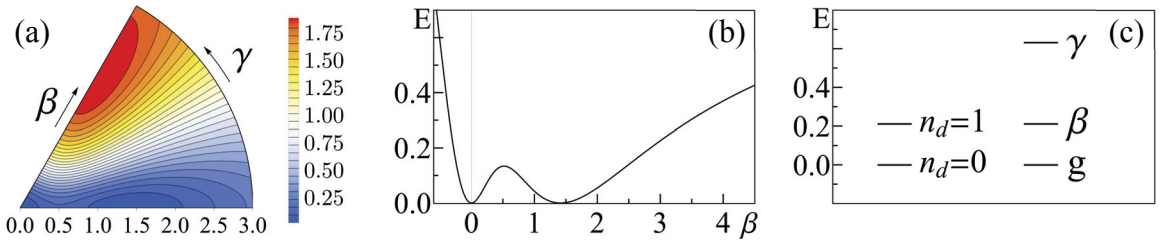

FIGURE 5. Spherical-prolate (S-P) shape coexistence. (a) Contour plots of the energy surface (7), (b) $\gamma=0$ sections, and (c) band-head spectrum, for the Hamiltonian $\hat{H}_{\rm PDS}$ of Eq. (33), with multiple U(5)-PDS and SU(3)-PDS. Adapted from [33].

The construction of Hamiltonians with several distinct partial dynamical symmetries, requires an extension of the previously discussed PDS algorithm. For that purpose, consider two DS chains of the IBM,

$$\mathrm{U}(6) \supset \mathrm{G}_1 \supset \mathrm{G}_2 \supset \ldots \supset \mathrm{SO}(3) \qquad |N,\, \lambda_1,\, \lambda_2,\, \ldots,\, L\rangle\,, \tag{27}$$

$$\mathrm{U}(6) \supset \mathrm{G}'_1 \supset \mathrm{G}'_2 \supset \ldots \supset \mathrm{SO}(3) \qquad |N,\, \sigma_1,\, \sigma_2,\, \ldots,\, L\rangle\,, \tag{28}$$

with different leading sub-algebras ($G_1 \neq G'_1$) and associated bases. We seek n-particle annihilation operators $\hat{T}_\alpha$ which satisfy simultaneously the following two conditions,

$$\hat{T}_\alpha |N, \lambda_1 = \Lambda_0, \lambda_2, \ldots, L\rangle \;=\; 0\,, \tag{29}$$

$$\hat{T}_\alpha |N, \sigma_1 = \Sigma_0, \sigma_2, \ldots, L\rangle \;=\; 0\,. \tag{30}$$

The states of Eq. (29) reside in the $\lambda_1 = \Lambda_0$ irrep of G_1, are classified according to the DS-chain (27), hence have good G_1 symmetry. Similarly, the states of Eq. (30) reside in the $\sigma_1 = \Sigma_0$ irrep of G'_1, are classified according to the DS-chain (28), hence have good G'_1 symmetry. The intrinsic Hamiltonian, $\hat{H}$, has the same form as in Eq. (10). Although G_1 and G'_1 are incompatible, relations (29)-(30) ensure that both sets of states are eigenstates of the same Hamiltonian. In general, $\hat{H}$ itself is not necessarily invariant under G_1 nor under G_2 and, therefore, its other eigenstates can be mixed with respect to both G_1 and G'_1. The collective Hamiltonian, $\hat{H}_c$, has the form as in Eq. (11), but now includes the Casimir operators of algebras which are common to both chains, and generate rotational splitting. The resulting complete Hamiltonian, $\hat{H}_{\rm PDS} = \hat{H} + \hat{H}_c$, Eq. (12), has both G_1-PDS and G'_1-PDS. The case of triple (or multiple) PDSs, associated with three (or more) incompatible DS-chains, is treated in a similar fashion.

In conjunction with quantum phase transitions, the two DS chains of Eqs. (27)-(28) describe the dynamics of different shapes, specified by equilibrium deformations (β_1, γ_1) and (β_2, γ_2). The derived PDS Hamiltonian has a potential surface with two degenerate minima, hence is qualified as a critical-point Hamiltonian. The two sets of solvable eigenstates, Eqs. (29)-(30), span the ground bands of the two shapes associated with the two minima. In what follows, we apply the above procedure to a variety of coexisting shapes and related multiple-PDSs in the IBM framework.

The U(5)-DS and SU(3)-DS chains, Eqs. (3) and (4), are relevant to spherical and prolate-deformed shapes. The construction of PDS Hamiltonian suitable for the coexistence of such shapes, follows the above procedure. The two-boson operator P_{2m} of Eq. (15) annihilates the states of the SU(3) irrep $(2N, 0)$ and the U(5) irrep, $n_d = 0$,

$$P_{2m}\,|N,\, (\lambda,\mu)=(2N,0),\, K=0,\, L\rangle \;=\; 0 \qquad\qquad L = 0, 2, 4, \ldots, 2N \tag{31}$$

$$P_{2m}\,|N,\, n_d = 0,\, \tau = 0,\, L = 0\rangle \;=\; 0\,, \tag{32}$$

and corresponds to the $\hat{T}_\alpha$ of Eqs. (29)-(30). The resulting PDS Hamiltonian is given by [32],

$$\hat{H}_{\rm PDS} = h_2\, P_2^\dagger \cdot \tilde{P}_2 + C\, \hat{C}_2[\mathrm{SO}(3)]\,, \tag{33}$$

and has a solvable prolate-deformed ground band with good SU(3) symmetry and a solvable spherical $L = 0$ ground state with good U(5) symmetry. $\hat{H}_{\rm PDS}$ has additional solvable SU(3) basis states $|N, (\lambda,\mu) = (2N - 4k, 2k) K = 2k, L\rangle$, which span the deformed $\gamma^k (K = 2k)$ bands, and an additional solvable U(5) basis state with $|N, n_d = \tau = L = 3\rangle$. Other eigenstates are mixed with respect to both U(5) and SU(3). Altogether, $\hat{H}_{\rm PDS}$ has U(5)-PDS coexisting with SU(3)-PDS. The corresponding energy surface, shown in Fig. 5, has degenerate spherical ($\beta_{\rm eq} = 0$) and prolate-deformed

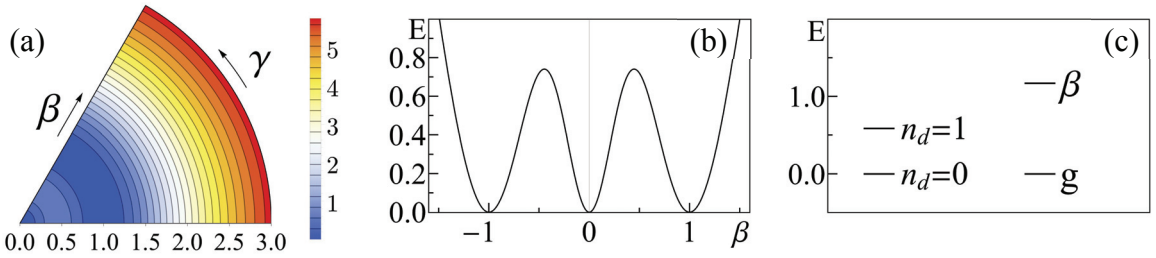

FIGURE 6. Spherical and γ-unstable deformed (S-G) shape coexistence. (a) Contour plots of the energy surface (7), (b) $\gamma = 0$ sections, and (c) bandhead spectrum, for $\hat{H}_{\rm PDS}$ of Eq. (36), with multiple U(5)-PDS and SO(6)-PDS. Adapted from [33].

($\beta_{\rm eq} = \sqrt{2}, \gamma_{\rm eq} = 0$) minima, separated by a barrier. $\hat{H}_{\rm PDS}$ thus qualifies as critical-point Hamiltonian. The normal modes involve β and γ vibrations about the deformed minimum and quadrupole vibrations about the spherical minimum. The bandhead spectrum associated with these modes, is shown in Fig. 5(c).

The U(5)-DS and SO(6)-DS chains, Eqs. (3) and (6), are relevant to spherical and γ-unstable deformed shapes. To construct a PDS Hamiltonian suitable for the coexistence of these shapes, we consider the operator $d_m R_0$ of Eq. (23), which annihilates the (τ, n_Δ, L) states of the SO(6) irrep $\sigma = N$ and the single $L = 0$ state of the U(5) irrep, $n_d = 0$,

$$d_m R_0 \,|N,\, \sigma = N,\, \tau,\, n_\Delta,\, L\rangle \;=\; 0 \qquad\qquad \tau = 0, 1, 2, \ldots, N \tag{34}$$

$$d_m R_0 \,|N,\, n_d = 0,\, \tau = 0,\, L = 0\rangle \;=\; 0\,. \tag{35}$$

The resulting PDS Hamiltonian is given by [33],

$$\hat{H}_{\rm PDS} \;=\; r_2\, R_0^\dagger \hat{n}_d R_0 + B\, \hat{C}_2[{\rm SO(5)}] + {\rm C}\, \hat{\rm C}_2[{\rm SO(3)}]\,, \tag{36}$$

and has a solvable γ-unstable deformed ground band with good SO(6) symmetry and a solvable spherical ground state with good U(5) symmetry. Other eigenstates are mixed with respect to both U(5) and SO(6). Altogether, $\hat{H}_{\rm PDS}$ has U(5)-PDS coexisting with SO(6)-PDS. The corresponding energy surface, shown in Fig. 6, is independent of γ, in accord with the SO(5) symmetry of the Hamiltonian. It has two degenerate minima at $\beta_{\rm eq} = 0$ and ($\beta_{\rm eq} = 1, \gamma_{\rm eq}$ arbitrary), separated by a barrier. $\hat{H}_{\rm PDS}$ thus qualifies as critical-point Hamiltonian. The normal modes involve β vibrations about the γ-unstable deformed minimum and quadrupole vibrations about the spherical minimum.

The SU(3)-DS and $\overline{\rm SU(3)}$-DS, Eqs. (4) and (5), are relevant to prolate and oblate shapes, respectively. The two chains have similar properties, but the classification of states is different. The ground band spans the irrep $(\lambda, \mu) = (2N, 0)$ [$(\bar{\lambda}, \bar{\mu}) = (0, 2N)$], in SU(3)-DS [$\overline{\rm SU(3)}$-DS], while the β and γ bands reside in the irrep $(\lambda, \mu) = (2N-4, 2)$ [$(\bar{\lambda}, \bar{\mu}) = (4, 2N-4)$]. In Figs. 7-8, we denote such prolate and oblate bands by (g_1, β_1, γ_1) and (g_2, β_2, γ_2), respectively. To construct a PDS Hamiltonian appropriate for prolate-oblate coexistence, we consider the three-boson operators: $s^\dagger P_0^\dagger$, $d_m^\dagger P_0^\dagger$, $W_{3m}^\dagger$, which satisfy

$$\begin{aligned}
&sP_0\,|N,\,(\lambda,\mu) = (2N,0),\,K=0,\,L\rangle = 0\,, \qquad &&sP_0\,|N,\,(\bar{\lambda},\bar{\mu}) = (0,2N),\,\bar{K}=0,\,L\rangle = 0\,,\\
&d_mP_0\,|N,\,(\lambda,\mu) = (2N,0),\,K=0,\,L\rangle = 0\,, \qquad &&d_mP_0\,|N,\,(\bar{\lambda},\bar{\mu}) = (0,2N),\,\bar{K}=0,\,L\rangle = 0\,,\\
&W_{3m}\,|N,\,(\lambda,\mu) = (2N,0),\,K=0,\,L\rangle = 0\,, \qquad &&W_{3m}\,|N,\,(\bar{\lambda},\bar{\mu}) = (0,2N),\,\bar{K}=0,\,L\rangle = 0\,.
\end{aligned} \tag{37}$$

Here $P_0^\dagger$ and $W_{3m}^\dagger$ are given in Eqs. (14) and 19), respectively. The PDS Hamiltonian is found to be [34],

$$\hat{H}_{\rm PDS} \;=\; h_0\, P_0^\dagger \hat{n}_s P_0 + h_2\, P_0^\dagger \hat{n}_d P_0 + \eta_3\, W_3^\dagger \cdot \tilde{W}_3 + C\, \hat{C}_2[{\rm SO(3)}] + \delta\, \hat{\rm C}_2[{\rm SU(3)}]\,. \tag{38}$$

The last term, with infinitesimally small δ, is needed to avoid an undesired invariance of the Hamiltonian with respect to a phase change of the s-boson [34]. $\hat{H}_{\rm PDS}$ has solvable prolate and oblate ground bands with good SU(3) and $\overline{\rm SU(3)}$ symmetry, respectively. Other eigenstates are mixed with respect to both SU(3) and $\overline{\rm SU(3)}$. Altogether, $\hat{H}_{\rm PDS}$ has SU(3)-PDS coexisting with $\overline{\rm SU(3)}$-PDS. The corresponding energy surface, shown in Fig. 7, has two degenerate minima at ($\beta_{\rm eq} = \sqrt{2}, \gamma_{\rm eq} = 0$) and ($\beta_{\rm eq} = \sqrt{2}, \gamma_{\rm eq} = \pi/3$), separated by a barrier. $\hat{H}_{\rm PDS}$ thus qualifies as a critical-point Hamiltonian. The normal modes involve β and γ vibrations about the respective deformed minima.

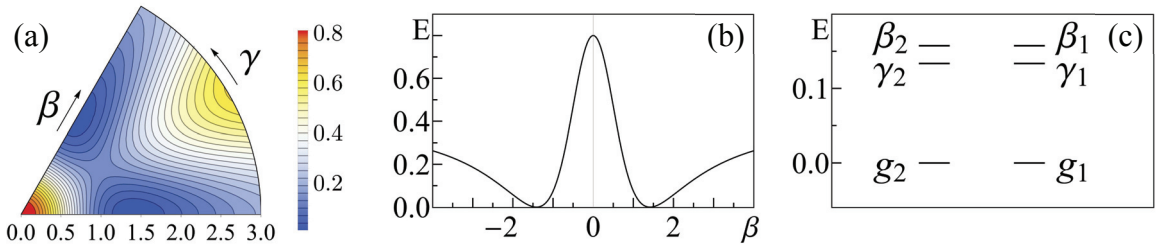

FIGURE 7. Prolate-oblate (P-O) shape coexistence. (a) Contour plots of the energy surface (7), (b) $\gamma=0$ sections, and (c) bandhead spectrum, for $\hat{H}_{\rm PDS}$ of Eq. (38), with multiple SU(3)-PDS and $\overline{\rm SU(3)}$-PDS. Adapted from [33].

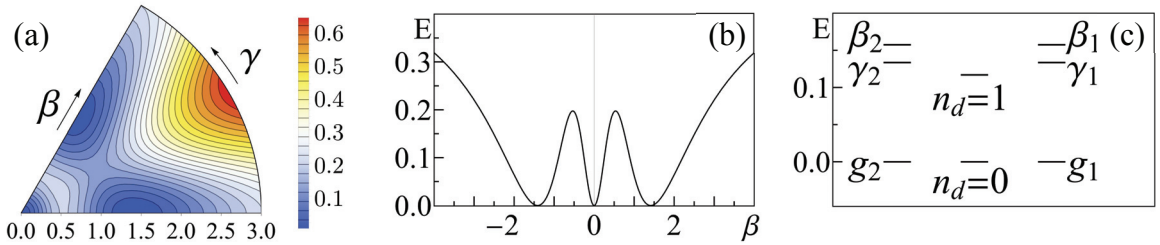

FIGURE 8. Spherical-prolate-oblate (S-P-O) shape coexistence. (a) Contour plots of the energy surface (7), (b) $\gamma=0$ sections, and (c) bandhead spectrum, for $\hat{H}_{\rm PDS}(h_0=0)$ of Eq. (38), with multiple U(5)-SU(3)-$\overline{\rm SU(3)}$ PDSs. Adapted from [33].

For $h_0=0$, the Hamiltonian of Eq. (38) exhibits multiple U(5), SU(3) and $\overline{\rm SU(3)}$ PDSs since the $d_m P_0$ and W_{3m} operators of Eq. (37), annihilate also the following U(5) basis state,

$$\begin{aligned} d_m P_0\,|N,\,n_d=0,\,\tau=0,\,L=0\rangle &= 0\,, \\ W_{3m}\,|N,\,n_d=0,\,\tau=0,\,L=0\rangle &= 0\,. \end{aligned} \tag{39}$$

Altogether, $\hat{H}_{\rm PDS}(h_0=0)$ has a solvable spherical ground state with good U(5) symmetry, in addition to solvable prolate and oblate ground bands with good SU(3) and $\overline{\rm SU(3)}$ symmetry. The corresponding energy surface, shown in Fig. 8, has three degenerate minima, at $\beta_{\rm eq}=0$ and ($\beta_{\rm eq}=\sqrt{2},\gamma_{\rm eq}=0,\pi/3$), separated by barriers. $\hat{H}_{\rm PDS}(h_0=0)$ thus qualifies as a critical-point Hamiltonian for triple coexistence of spherical, prolate and oblate shapes. In addition to β and γ vibrations, the normal modes involve also quadrupole vibrations about the spherical minimum.

In all cases of shape-coexistence and multiple-PDSs considered above, one can obtain analytic expressions of quadrupole moments and transition rates for the remaining solvable states, which are the observables most closely related to the nuclear shape. These expressions can be used as signatures and tests for the underlying PDSs. The purity and good quantum numbers of these selected states, enable the derivation of symmetry-based selection rules for $E2$ and $E0$ decays and, as shown Fig. 9, the subsequent identification of isomeric states.

Partial dynamical symmetries have also been identified in coupled systems with $U_1(m)\otimes U_2(n)$ spectrum generating algebras. This includes, partial F-spin symmetry [35] in the proton-neutron version of the interacting boson model (IBM-2) [1] of even-even nuclei, and $\rm SO_{B+F}(6)$ partial Bose-Fermi symmetry [36] in the interacting boson-fermion model (IBFM) of odd-mass nuclei [2]. Hamiltonians with PDS are not completely regular nor fully chaotic. As such they are relevant to the study of mixed systems with coexisting regularity and chaos [37, 38, 39].

ACKNOWLEDGMENTS

It is a pleasure and honor to dedicate this contribution to Francesco Iachello on the occasion of his retirement. Franco: "a one-man center of theoretical physics", a rare combination of true scholar, innovative scientist and friend. I vividly recall and cherish many "blackboard hours" of in-depth discussions, thoughtful guidance, impact and inspiration. Segments of the reported results were obtained in collaboration with N. Gavrielov (HU), J. E. García-Ramos (Huelva) and P. Van Isacker (GANIL). This work is supported by the Israel Science Foundation (Grant 586/16).

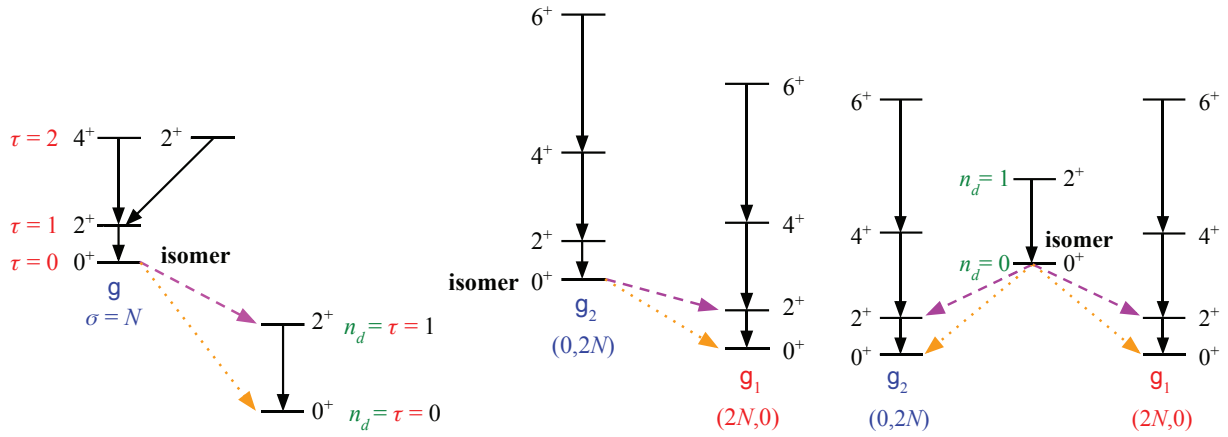

FIGURE 9. Signatures of multiple U(5)-SO(6) PDSs (left panel), SU(3)-$\overline{\text{SU(3)}}$ PDSs (center panel), and U(5)-SU(3)-$\overline{\text{SU(3)}}$ PDSs (right panel), relevant to S-G, P-O and S-P-O shape coexistence, respectively. The rates for the strong intraband $E2$ transitions (solid lines) are known analytically. Retarded $E2$ (dashes lines) and $E0$ (dotted lines) decays identify isomeric states.

REFERENCES

[1] F. Iachello, and A. Arima, *The Interacting Boson Model*, Cambridge Univ. Press, Cambridge, 1987.
[2] F. Iachello, and P. Van Isacker, *The Interacting Boson-Fermion Model*, Cambridge Univ. Press, Camb., 1991.
[3] F. Iachello, and R. D. Levine, *Algebraic Theory of Molecules*, Oxford Univ. Press, Oxford, 1995.
[4] R. Bijker, F. Iachello, and A. Leviatan, *Ann. Phys. (NY)* **236**, 69 (1994).
[5] F. Iachello, *Lie Algebras and Applications*, Berlin Heidelberg: Springer-Verlag, 2015.
[6] A. Arima, and F. Iachello, *Phys. Rev. Lett.* **35**, 1069 (1975).
[7] A. Arima, and F. Iachello, *Ann. Phys. (N.Y.)* **99**, 253 (1976).
[8] A. Arima, and F. Iachello, *Ann. Phys. (N.Y.)* **111**, 201 (1978).
[9] A. Arima, and F. Iachello, *Ann. Phys. (N.Y.)* **123**, 468 (1979).
[10] J.N. Ginocchio, and M.W. Kirson, *Phys. Rev. Lett.* **44**, 1744 (1980)
[11] A.E.L. Dieperink, O. Scholten, and F. Iachello, *Phys. Rev. Lett.* **44**, 1747 (1980).
[12] A. Leviatan, *Prog. Part. Nucl. Phys.* **66**, 93 (2011).
[13] Y. Alhassid, and A. Leviatan, *J. Phys. A* **25**, L1265 (1992).
[14] J. E. García-Ramos, A. Leviatan, and P. Van Isacker, *Phys. Rev. Lett.* **102**, 112502 (2009).
[15] M.W. Kirson, and A. Leviatan, *Phys. Rev. Lett.* **55**, 2846 (1985)
[16] A. Leviatan, *Ann. Phys. (N.Y.)* **179**, 201 (1987).
[17] A. Leviatan, *Phys. Rev. Lett.* **77**, 818 (1996).
[18] A. Leviatan, and I. Sinai, *Phys. Rev. C* **60**, 061301(R) (1999).
[19] R. F. Casten, R. B. Cakirli, K. Blaum, and A. Couture, *Phys. Rev. Lett.* **113**, 112501 (2014).
[20] A. Couture, R. F. Casten, and R. B. Cakirli, *Phys. Rev. C* **91**, 014312 (2015).
[21] A. Leviatan, J. E. García-Ramos, and P. Van Isacker, *Phys. Rev. C* **87**, 021302(R) (2013).
[22] A. Aprahamian *et al.*, *Phys. Rev. C* **98**, 034303 (2018).
[23] N. Gavrielov, A. Leviatan, J. E. García-Ramos, and P. Van Isacker, *Phys. Rev. C* **301**, 031302(R) (2018).
[24] R. Gilmore, and D.H. Feng, *Nucl. Phys. A* **301**, 189 (1978).
[25] L. Carr, ed., *Understanding Quantum Phase Transitions*, CRC Press, Boca Raton, FL, 2011.
[26] P. Cejnar, J. Jolie, and R.F. Casten, *Rev. Mod. Phys.* **82**, 2155 (2010).
[27] F. Iachello, *Rivista del Nuovo Cimento* **34**, 617 (2011).
[28] F. Iachello, A. Leviatan, and D. Petrellis, *Phys. Lett. B* **705**, 379 (2011).
[29] D. Petrellis, A. Leviatan, and F. Iachello, *Ann. Phys. (N.Y.)* **326**, 926 (2011).
[30] F. Iachello, *Phys. Rev. Lett.* **85**, 3580 (2000).
[31] F. Iachello, *Phys. Rev. Lett.* **87**, 052502 (2001).
[32] A. Leviatan, *Phys. Rev. Lett.* **98**, 242502 (2007).
[33] A. Leviatan, and N. Gavrielov, *Phys. Scr.* **92**, 114005 (2017).
[34] A. Leviatan, and D. Shapira, *Phys. Rev. C* **93**, 051302(R) (2016).
[35] A. Leviatan and J.N. Ginocchio, *Phys. Rev. C* **61**, 024305 (2000).
[36] P. Van Isacker, J. Jolie, T. Thomas, and A. Leviatan, *Phys. Rev. C* **92**, 011301(R) (2015).
[37] N. Whelan, Y. Alhassid, and A. Leviatan, *Phys. Rev. Lett.* **71**, 2208 (1993).
[38] A. Leviatan, and N.D. Whelan, *Phys. Rev. Lett.* **77**, 5202 (1996).
[39] M. Macek. and A. Leviatan, *Ann. Phys. (N.Y.)* **351**, 302 (2014).